CHAPTER-V

Electrical Properties Of Mn - Oxide Films :

C H A P T E R - V

ELECTRICAL PROPERTIES OF Mn-OXIDE FILMS

5.1 Introduction :

Electrical characterization is essential in order to understand the charge transport in the semiconducting materials. Dark conductivity and thermoelectric power measurement are important to get an idea about the activation energy of the carriers and mobility, situation of energy levels and type of particular semiconductor. For the measurement of dark conductivity the thickness measurement of the film is essential. In this chapter, the effects of concentration, substrate temperature and spray rate on electrical properties and thickness are reported. Also the variation of thickness of the film deposited on conducting and non-conducting substrates was studied.

5.2 Experimental :

To study transport properties, the following experimental setups were used and described one by one.

5.2.1 Experimental setup for Electrical Properties :

a) Dark Conductivity Measurement

The dark conductivity of the film was measured with the help of experimental setup designed and fabricated in our laboratory. This is schematically shown in fig. 5.1/1/. The two brass plates of the same size (10x5x0.5 cm) are groved at centre of asbestos sheet and fixed with the help of screw to fix the heating element (Toni 60W). Two heating elements were fixed parallel in order to achieve the uniform

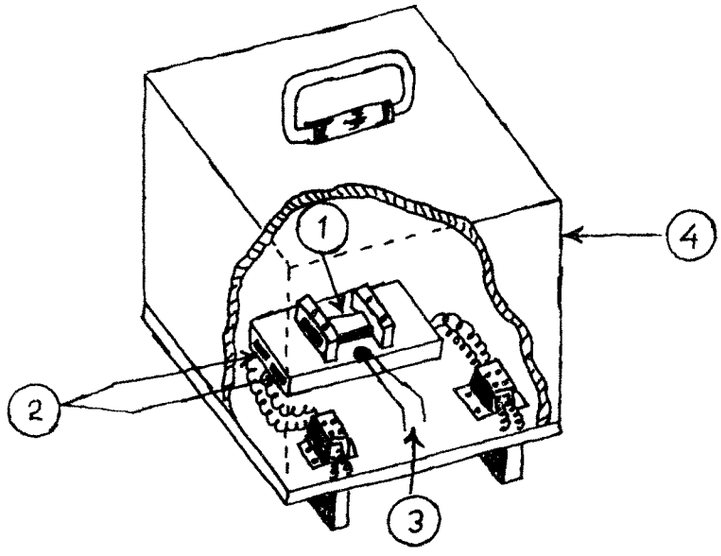

Fig. 5.1 Schematic diagram of the conductivity unit.
(1) Sample (2) Heaters (3) Thermocouple (4) Shield.

temperature in required area. The sample holder was at the top of the upper plate. The film of size 2.3x0.5 cm on glass substrates were used. Press contacts were made to the films with copper strips which are soldered by an electrical wire to provide an external electrical connections. Silver paste was used to get good contact. The mica sheet was placed on the brass plate to avoid the contact between the film and plate. Thermal radiations are reduced by using the metal cover with asbestoss sheet.

Temperature was measured with Chromel-Alumel thermocouple (24 gauge) which was fixed at the centre of the sample. And temperature was recorded on pla-digital millivoltmeter, DPM-10. The regulated power supply unit (T.P.S.U.) Aplab was used for passing the current through the films. The potential drop across the film was measured with the help of Digitl multimeter (Pla-DM-148-B) and current through the film was measured with Aplab FET nanoammeter (TFM-19).

b) Thermoelectric Power (TEP) Measurement.

A schematic diagram for the thermoelectric power measurement is shown in fig.5.2(a) and 5.2(b). A brass block was used as a sample holder. The typical shape [as shown in fig.5.2(c)] of the block gives the uniform temperature gradient along the length of the sample holder. This sample holder was fixed on porcellin base. The films of size 2.3x0.5 cm on glass substrate were used for TEP measurement. The press contacts were made to the film with copper strips and external electrical connection is made by soldering an

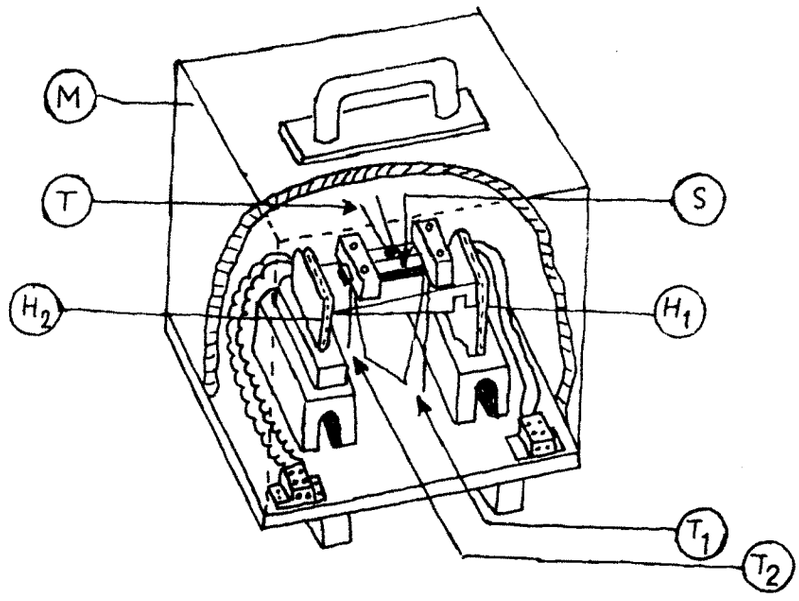

Fig. 5.2(a) Schematic diagram of thermoelectric power unit.
S - sample M - metal shield T - mean temperature
H_1,H_2 - heaters T_1,T_2 - Differential thermocouple junction.

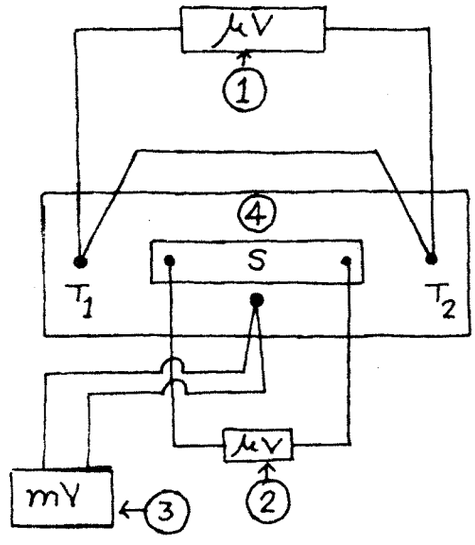

Fig. 5.2(b) Circuit diagram for thermoelectric power measurement.

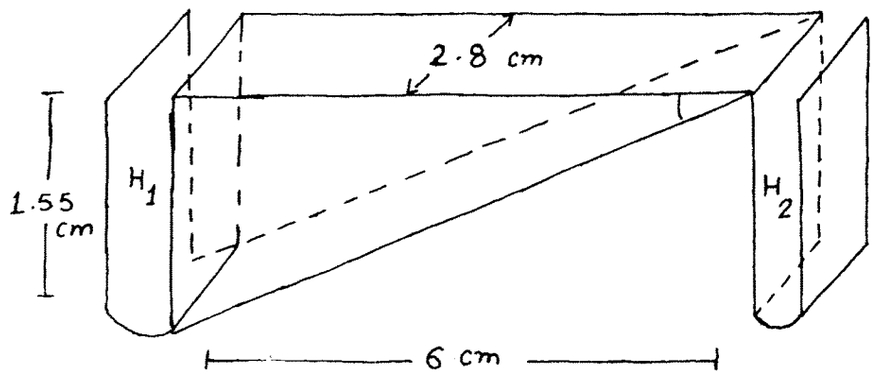

Fig. 5.2(c) Design of specially made sample holder.

electric wire to these strips. Silver point was used for perfect contacts. The two miniheaters (H_1 or H_2) with different heating capacity are used for heating the sample. A metal cover was used for shielding the TEP unit.

A differential Chromel-Alumel thermocouple was used to measure the temperature gradient across the sample and mean temperature. The differential thermocouple voltage was measured with Philips D.C. microvoltmeter (PP 9004) and mean temperature was measured with Pla-digital voltmeter (DPM-10). The thermoelectric voltage was measured by using VASAVI digital microvoltmeter (VMV-15).

5.2.2 Experimental setup for Thickness Measurement :

The thickness of the film was determined by the method of weighing, in which the area and weight of the films were measured/2/. The film thickness was measured by using the relation

$$t = \frac{m}{\rho \times A} \qquad \ldots\ldots (5.1)$$

Where, m is the weight of the film, A is the area of the film and ρ is the density of the material deposited.

5.3 Results and Discussion :

5.3.1 Dark Conductivity :

The concentration, substrate temperature and spray rate affect the dark conductivity. Fig.s 5.3, 5.4 and 5.5 show the variation of log R versus 1/T at different concentrations (S_1, $S_{0.5}$, $S_{0.25}$ and $S_{0.1}$) substrate temperatures (S_{375}, S_{425} and S_{400}), and spray rates (S_6, S_8, S_{10} and S_{12}) respectively.

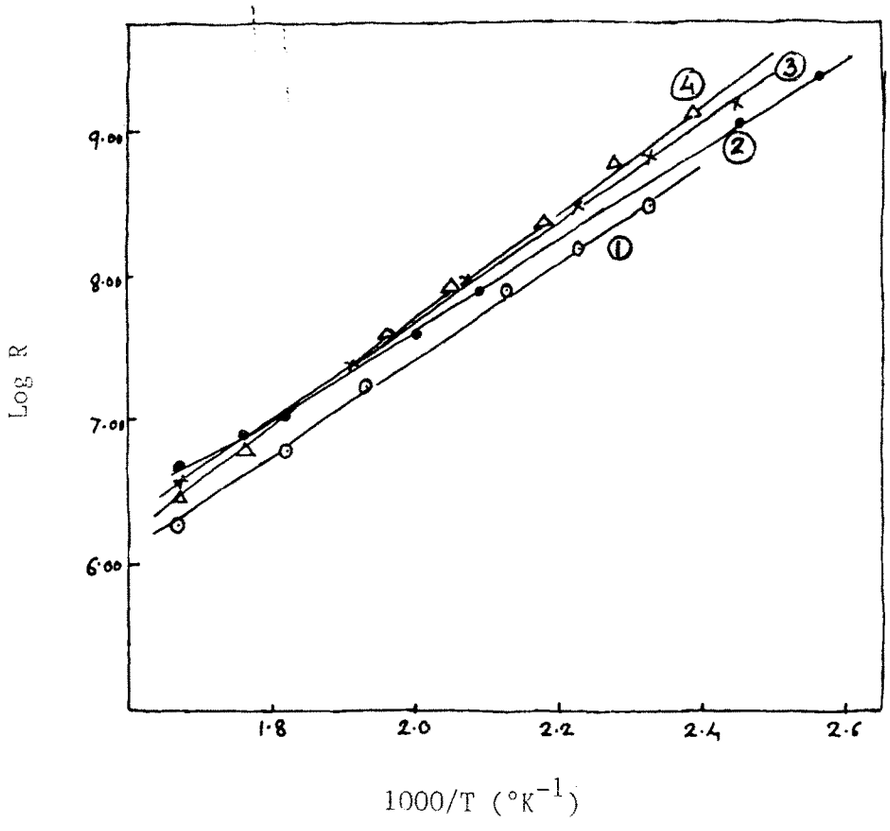

Fig. 5.3 Temperature dependence of log R for typical films prepared with different concentrations of spraying solution.
(1) 0.25 M (2) 1 M (3) 0.1 M (4) 0.5 M.

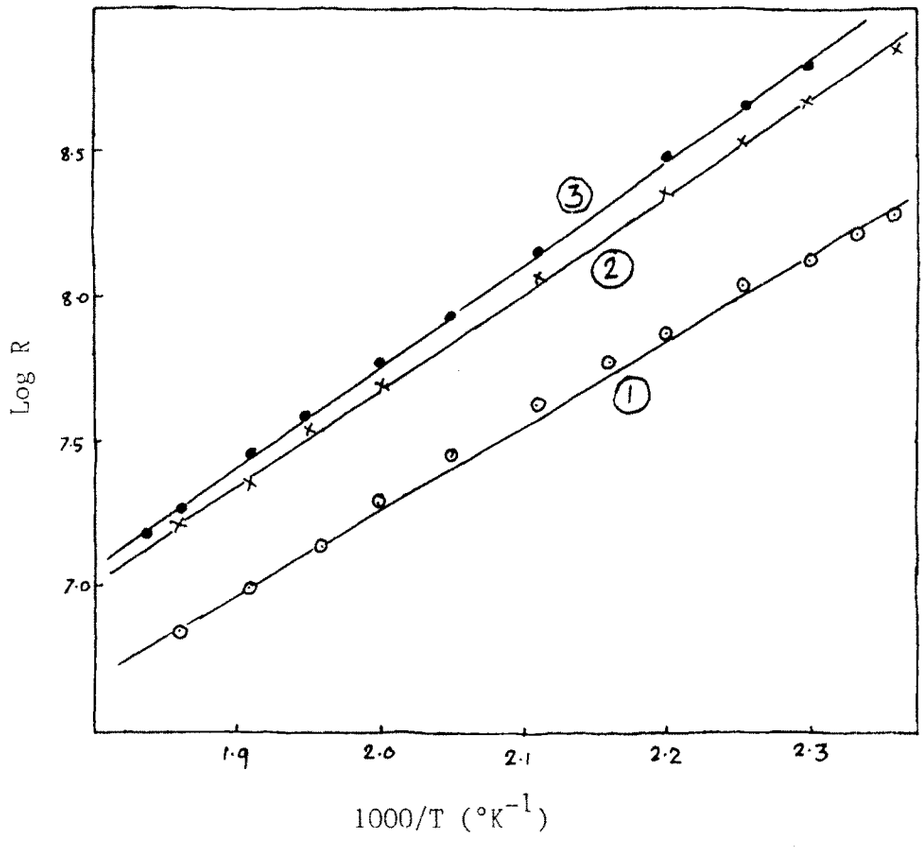

Fig. 5.4 Temperature dependence of log R for films prepared of different substrate temperatures.
(1) 400°C (2) 425°C (3) 375°C.

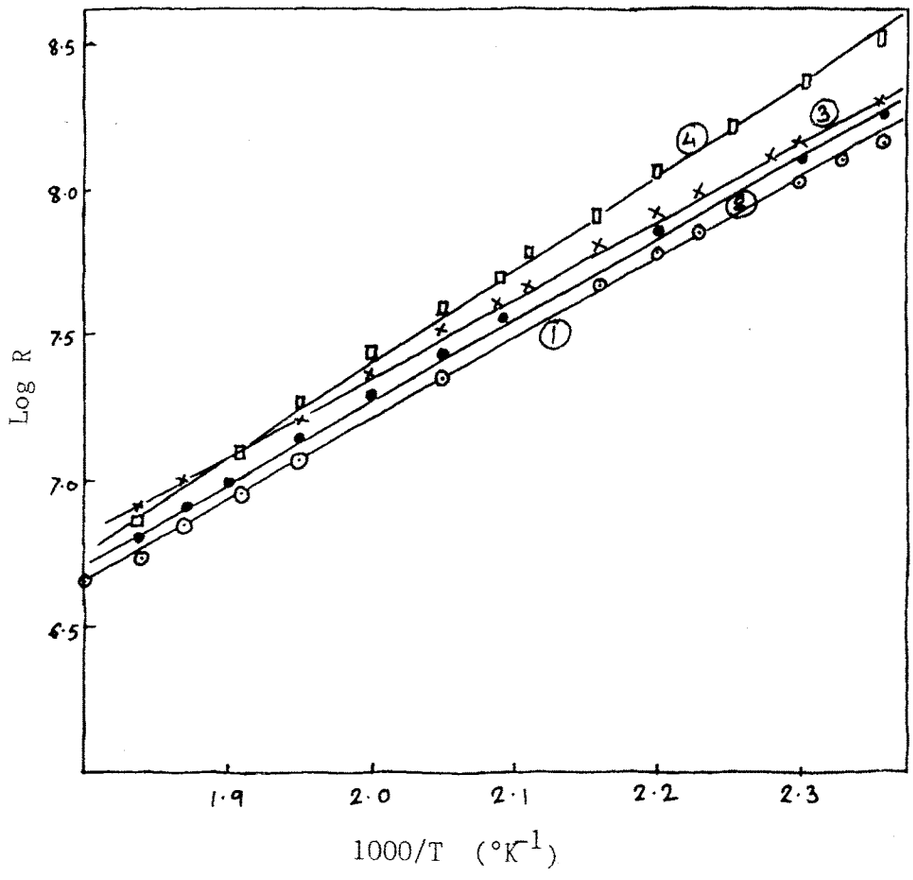

Fig. 5.5 Temperature dependence of log R for films prepared with different spray rates .
(1) 8 cc/min (2) 10 cc/min (3) 12 cc/min (4) 6 cc/min.

All these plots are linear. These graphs show that the log R values are less for 0.25 M concentration, 400°c substrate temperature and 8 cc/min spray rate as compared to the log R values corresponding to other concentrations (see $S_{0.1}$, $S_{0.5}$, S_1), substrate temperatures (S_{375}, S_{425}) and spray rate (S_6, S_{10}, S_{12}) respectively.

Fig.s 5.6, 5.7 and 5.8 show the dark conductivity as a function of concentration, substrate temperature and spray rate respectively. The plot of conductivity versus concentration (fig. 5.6) shows that the conductivity increases with decrease in concentration, attains the maximum value at 0.25M concentration and further decrease in molarity of initial solution conductivity decreases. The variation of conductivity with substrate temperature (fig.5.7) shows that the conductivity increases with substrate temperature. It attains maximum value at 400°c and then further decreases with increasing substrate temperature. The plot of conductivity versus spray rate (fig. 5.8) shows that the conductivity slightly decreases for the spray rate 8 cc/min as compared to the spray rate 6 cc/min. And it increases with the increase in spray rate.

Electrical conductivity measurements are made to investigate the conduction mechanism in oxides. The conduction mechanism in metal oxides differs fundamentally from that found in ease of Germanium and Silicon because these metal oxides possess partially filled 'd' levels of cations. The

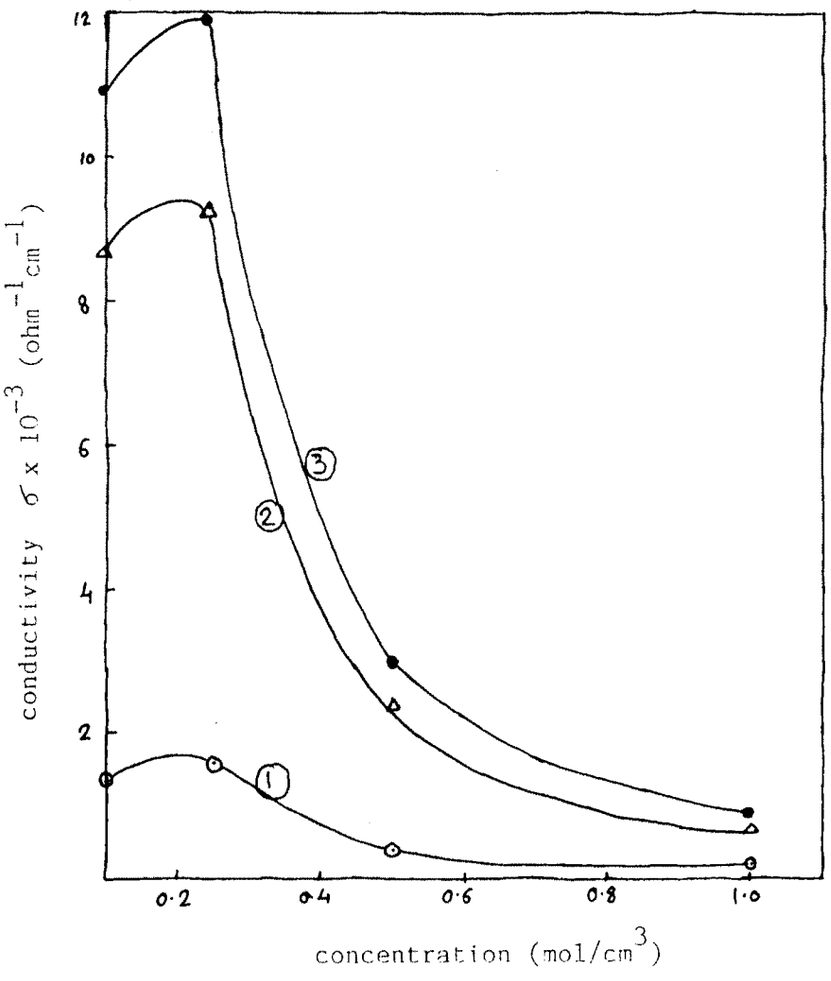

Fig. 5.6 Plot of conductivity versus concentration of spraying solution for different mean temperatures.
(1) 508 ^{o}K (2) 568 ^{o}K (3) 578 ^{o}K

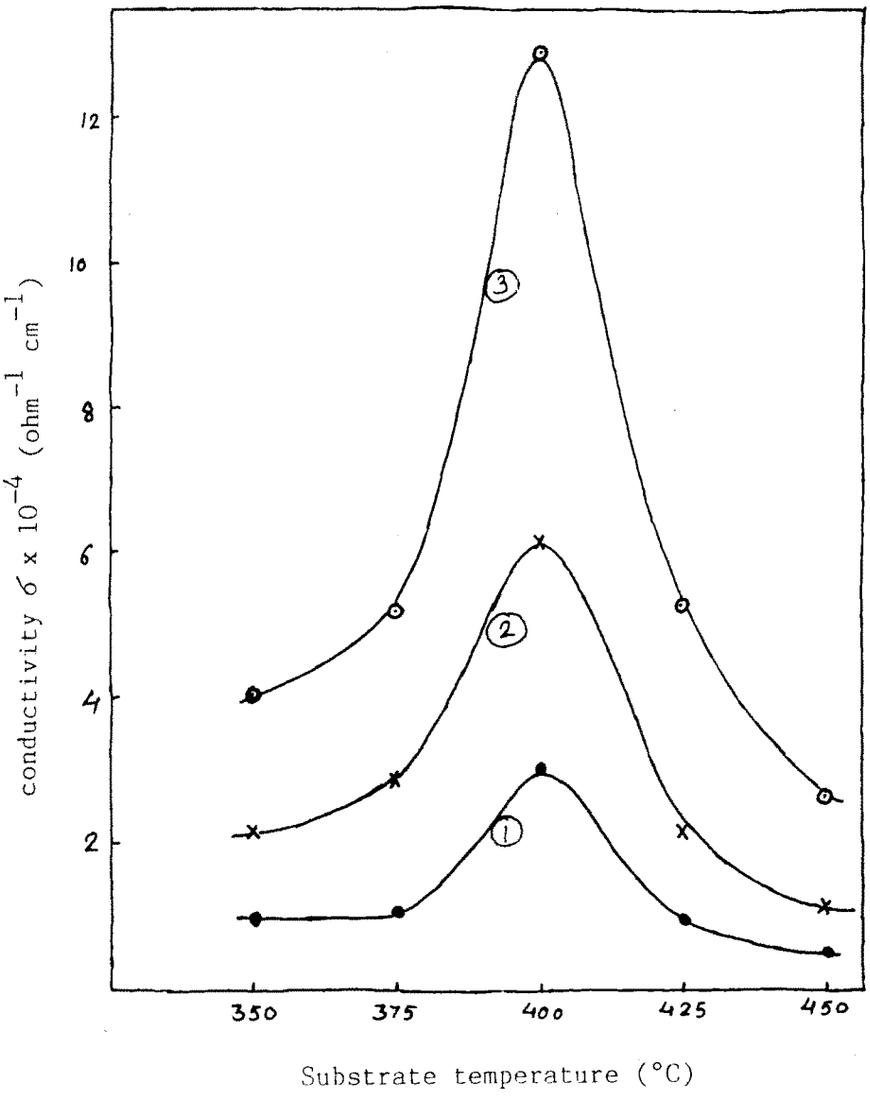

Fig. 5.7 Variation of conductivity with substrate temperature for different mean temperatures (1) 473 °K (2) 498°K (3) 523.°K

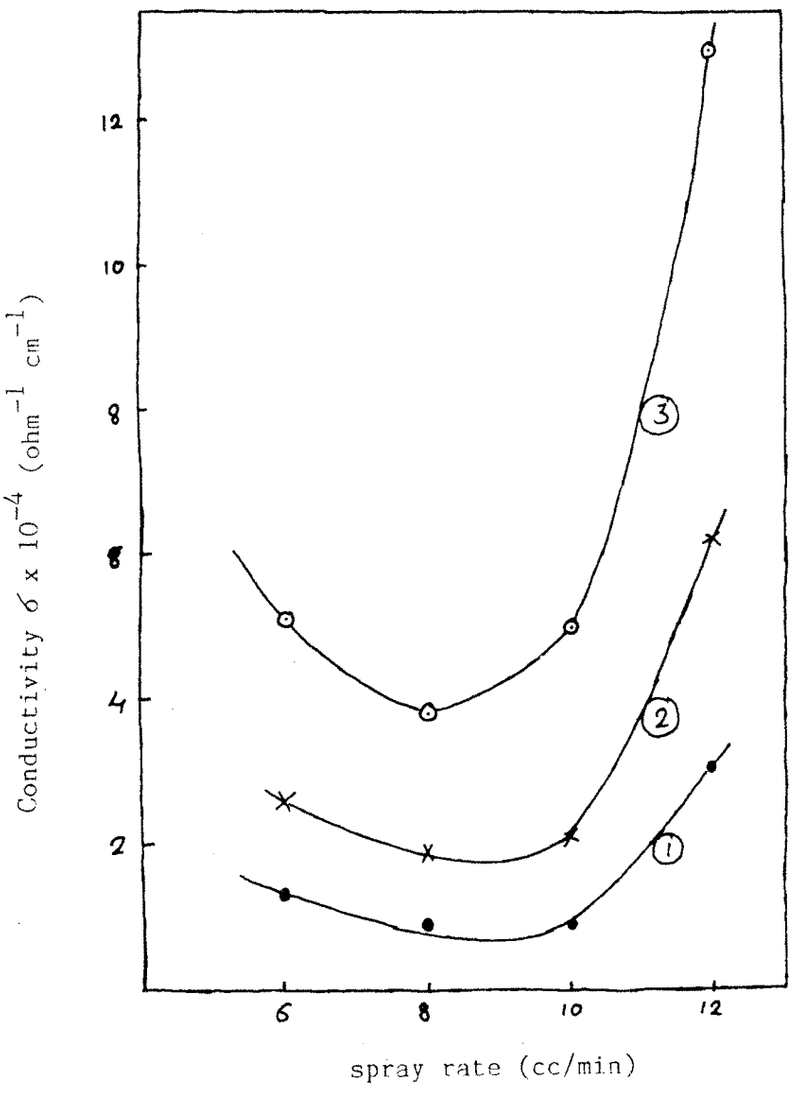

Fig. 5.8 Variation of conductivity with spray rate for different mean temperatures (1) 473°K(2) 498°K(3) 523°K

electrical conductivity of a '3d' compound gives a complex conduction mechanism due to the complex electronic structures of these compounds/3/. In these compounds '2s' and '2p' oxygen orbitals strongly overlap the 4s and 4p orbitals of the3d transition metal ions. Thus a strong hybridization results which gives a large energy band gap between top of the '4s' and '4p' band. The tenfold degeneracy of the 3d bands which lies among the 2p, 4s, 4p bands is partially removed by crystal field and exchange splitting. The filled '2p' band of oxygen and '3d' band of metal ions are responsible for conduction/4/.

In this subsection resistance for all films is measured in the temperature range between 300°K to 550°K. The conductance calculated from the resistance shows increase in its value with rise in temperature indicates the semiconducting behaviour of Mn-oxide films. This variation of conductance with temperature is useful in intrisic region to determine the band gap Eg of the material deposited/5/. The graphs of log R against 1/T for different concentrations, substrate temperatures and spray rates are straight lines. This linear nature of plots agrees with theoretical plot as given in the theory of transport properties of transition metal oxides. Resistivity of tetragonal Mn_3O_4 was reported by Sarkar et al. /6/. The value of activation energy is calculated by employing the relation

$$R = R_o \exp\left(- \frac{\Delta Ea}{kT} \right) \qquad \ldots\ldots (5.2)$$

where R is the resistance at temperature T, R_o constant

in ohm, Ea is activation energy in electron volt, k is Boltzman's constant in electron volts per degree, T is the absolute temperature in degree Kelvin.

The values of activation energy are determined from the slopes of plots shown in fig.s 5.3, 5.4 and 5.5. The table 5.1 shows activation energies corresponding to different concentrations, substrate temperatures and spray rates. The activation energy decreases with decrease in concentration. The value of activation energy for 0.25M concentration is in good agreement with the activation energy of Mn_2O_3 as reported by Subba Rao et al/7/ in bulk form. This shows that for 0.25M concentration the percentage of Mn_2O_3 in Mn-oxide [$Mn_3O_4 \longrightarrow MnO.MnO_3$] is more which is supported by structural property as discussed in chapter IV. As only for 10 and 12 cc/min spray rates films are uniform on conducting and non-conducting glass substrates, compare the activation energy of these films only. The comparison shows that the activation energy is nearly equal to the activation energy of Mn_2O_3 for the film deposited with spray rate 12 cc/min. The table 5.1 shows that the activation energy for 400 and 425°c substrate temperatures is closed to the activation energy of Mn_2O_3, but conductivity is more at 400°c than 425°c as shown in fig. 7.

The lower conductivity at higher concentration (fig.5.6 may be attributed to (a) incomplete oxidation of initial ingradient (b) poor crystallinity of films. However lower conductivity for a film prepared with 0.1M concentration may

Table No. 5.1

Activation Energy Chart

Concentration in mol/cm^3	Activation Energy in eV
1	0.84
0.5	0.73
0.25	0.66

Spray Rate in cc /min.	Activation Energy in eV
6	0.65
8	0.55
10	0.78
12	0.57

Substrate Temperature in °C	Activation Energy in eV
350	0.15
375	0.76
400	0.58
425	0.67
450	0.16

be due to discontinuous nature of the film. Fig. 5.7 shows maximum conductivity for a film deposited at 400°c substrate temperature. This may be due to high percentage of Mn_2O_3 in Mn-oxide. The study of structural properties of Mn-oxide films (chapter IV) shows higher percentage of Mn_2O_3 for 0.25M concentration and 400°C substrate temperature. In Mn_3O_4 the percentage of Mn_2O_3 is responsible for conduction as in Mn_3O_4 the conduction may be due to transformation of Mn_3O_4 to more strongly oxidized forms i.e. α-Mn_2O_3 or /βMnO_2/8/. OR the maximum conduction may be due to maximum nonstoichiometric defects at 400°c as compared to the other substrate temperatures. In transition metal oxides the defect is a metal deficiency defect. Crystals with metal deficiency defects are semiconductors due to the moving of an electron from A^+ion (Mn^+ion) to an A^{2+}ion(Mn^{2+}ion), i.e. an apparent movement of A^{2+}. This is called P-type conduction.

The maximum conductivity at 12 cc/min spray rate (fig. 5.8) may be due to better crystallinity for the particular film (0.25M concentration and 400°c substrate temperature).

5.3.2 Thermoelectric Power :

It is equally important to study the thermoelectric power to know the conduction mechanism in transition metal oxides. The thermoelectric power, TEP or α , for a polycrystalline semiconductor can be defined in a formal way as the ratio of the measured Seebeck Voltage to the temperature difference/9/. It is expressed by the relation

$$\alpha = \frac{\Delta V}{\Delta T} \qquad \ldots\ldots\ldots \quad (5.3)$$

where ΔV is the thermal voltage and ΔT is the temperature difference across the semiconductor.

It is also known as Seebeck coefficient. The temperature difference causes a migration of the majority carriers. Transport of carriers from hot end to cold end creates an electric field which gives rise to thermal voltage (ΔV). This thermally generated voltage is directly proportional to temperature difference created across the semiconductor. One can determine from the sign of thermoelectric power whether electrons or holes make the domient contribution to the conduction mechanism. Density of majority charge carriers is also determined from thermoelectric power (α).

The fig.s 5.9 and 5.10 show the variation of thermoelectric power with mean temperature for different concentrations and for two particular substrate temperatures. In both the plots thermoelectric power increases with increase in mean temperature. But after a particular temperature the thermoelectric power decreases. The fig.s 5.9 and 5.10 show that TEP is higher for the films $S_{0.25}$ and S_{400} respectively.

Thermoelectric power studies show that the electrons make domient contribution to the conduction process. Most of the literature on conductivity and thermoelectric power have been predicted that conduction mechanism in oxide semiconductors could not be interpreted in terms of assumption

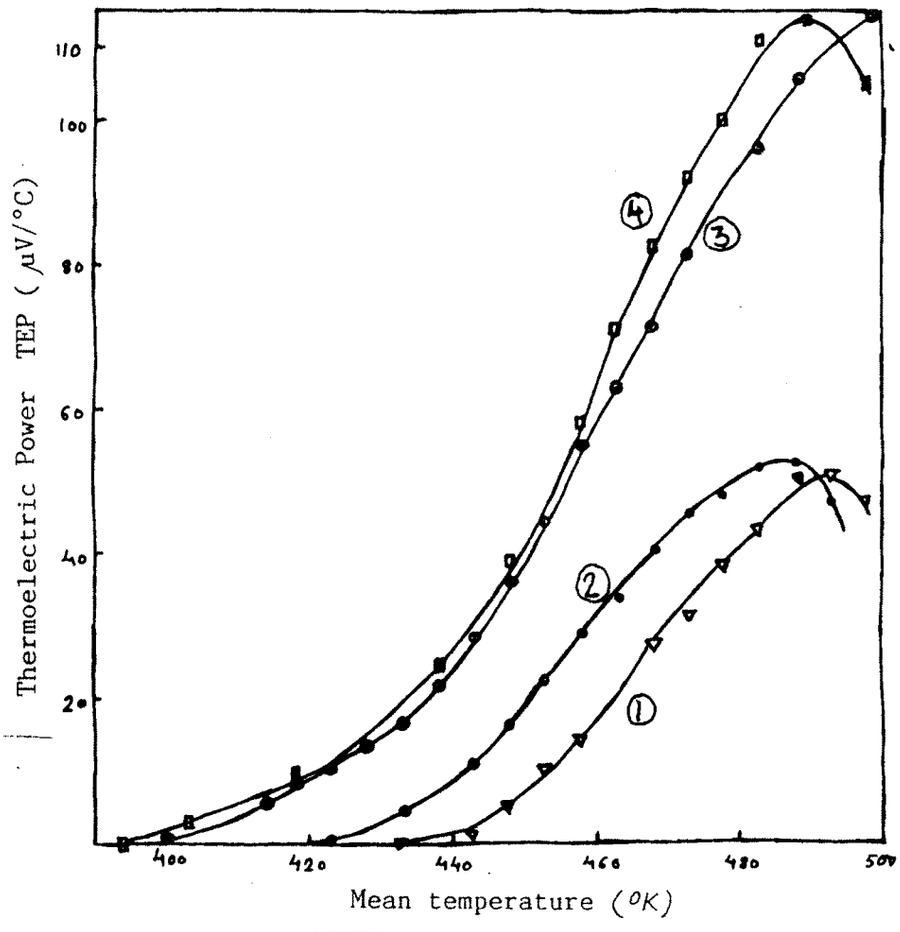

Fig. 5.9 Variation of thermoelectric power with mean temperature for films deposited with different concentrations of spraying solution (1)0.5 M (2) 0.1 M (3) 1 M (4) 0.25 M.

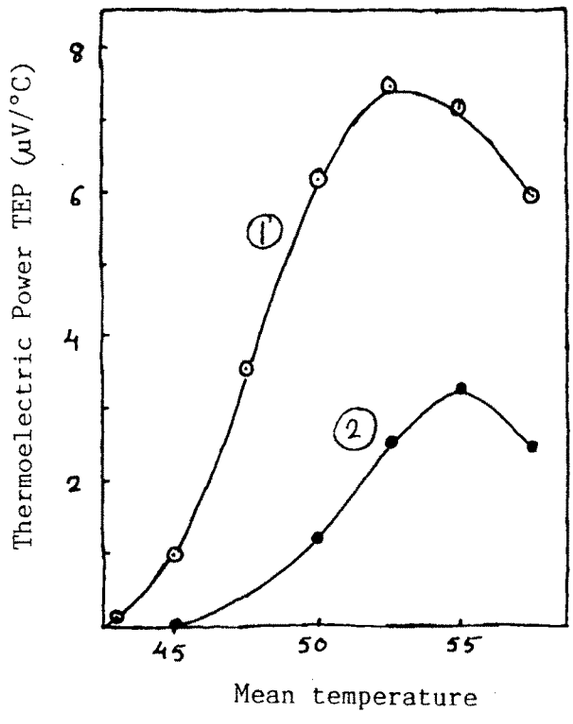

Fig. 5.10 Variation of thermoelectric power as a function of mean temperature for films prepared at different substrtate temperatures. (1) 400°C (2) 450°C

of simple band theory of semiconductors. Thus two alternative models have been put forth to explain conduction phenomena in these semiconductors/10,11/. First model is concerned with the transition between 'd' levels of 'Mn' ions. This was consistent with low mobility carriers. Since Mn-oxide is metal deficient oxide, the probability of transfer of electrons from metal to metal is more. Another model involves sp to sp excitation. Since this model is concerned with transfer of electron from 'O' ion to 'O' ion, it is assumed to unfit for Mn-oxide.

Here thermoelectric power (TEP or α) is measured in dark as a function of temperature in the range between 300°K to 500°K for all samples. From the polarity of the thermo e.m.f. (negtive at hot end) it is found that all films studied are of p-type. Similar observations are made by Subba Rao/7/ and Sykora/12/. The thermoelectric power for a p-type material is given by the relation

$$\alpha = \frac{k}{e} \left[A + \ln \frac{Ev}{P} \right]$$

The increase in thermoelectric power with mean temperature may be attributed to decrease in concentration of the free holes at higher temperature.

5.3.3 Thickness

In the present work the effect of concentration, substrate temperature and spray rate on thickness was studied. Also the variation between thickness of film deposited on conducting and nonconducting substrates keeping all other

parameters constant was studied. Thickness of the films was estimated by using the relations 5.1 , when we assume the density of the deposit is 4.5 gm/cm^3. Figs.5.11,5.12 and 5.13 show the variation of thickness with the concentration of spraying solutions, substrate temperatures and spray rates respectively. The thickness increases with the concentration as shown in fig. 5.11. The thickness slowly increases with substrate temperature (fig.5.12). In fig. 5.13 the thickness is maximum for the spray rate 8cc/min and it decreases for lower and higher spray rates than 8cc/min, for conducting as well as nonconducting glass substrates.

The increased in thickness with concentration may be attributed to increase availability of metal ions for oxide formation with concentration. While the increase in thickness with increase in substrate temperature/13/ may be attributed to more increase in decomposition rate with substrate temperature than increase in evaporation rate of the initial products. It is found that the thickness of the film deposited on conducting glass substrate is smaller than that of films deposited on nonconducting glass substrates. These results are in good agreement with the results reported by others /14,15/. The small film thickness on conducting glass may be due to the relatively rough surface of the FTO film. Further the decrease in the film thickness with decrease in spray rate may be attributed to the increase in evaporation of the initial ingradient due to large time of deposition for lower spray rates. On the other hand the decrease in the

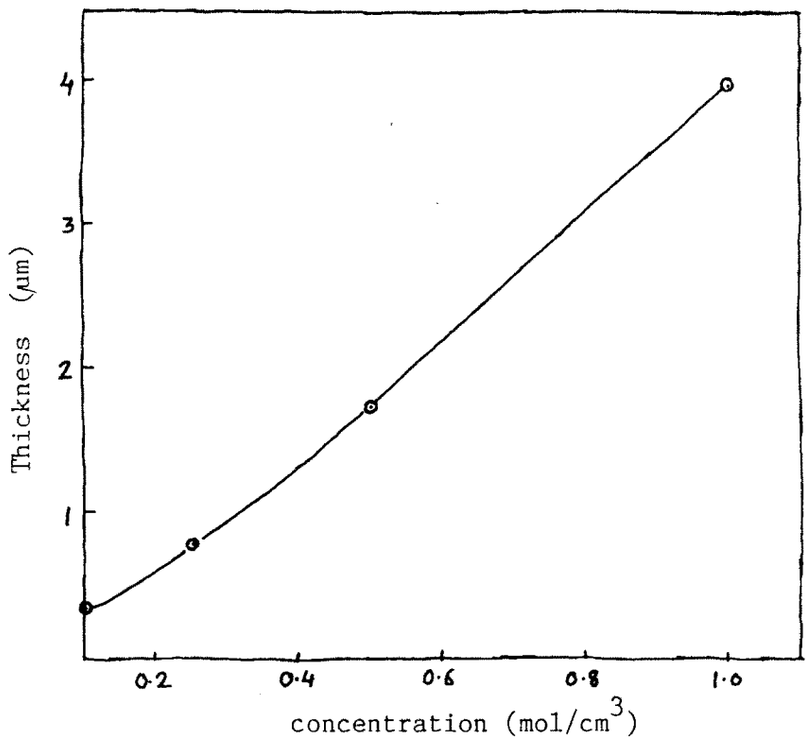

Fig. 5.11 Plot of film thickness versus concentration of spraying solution.

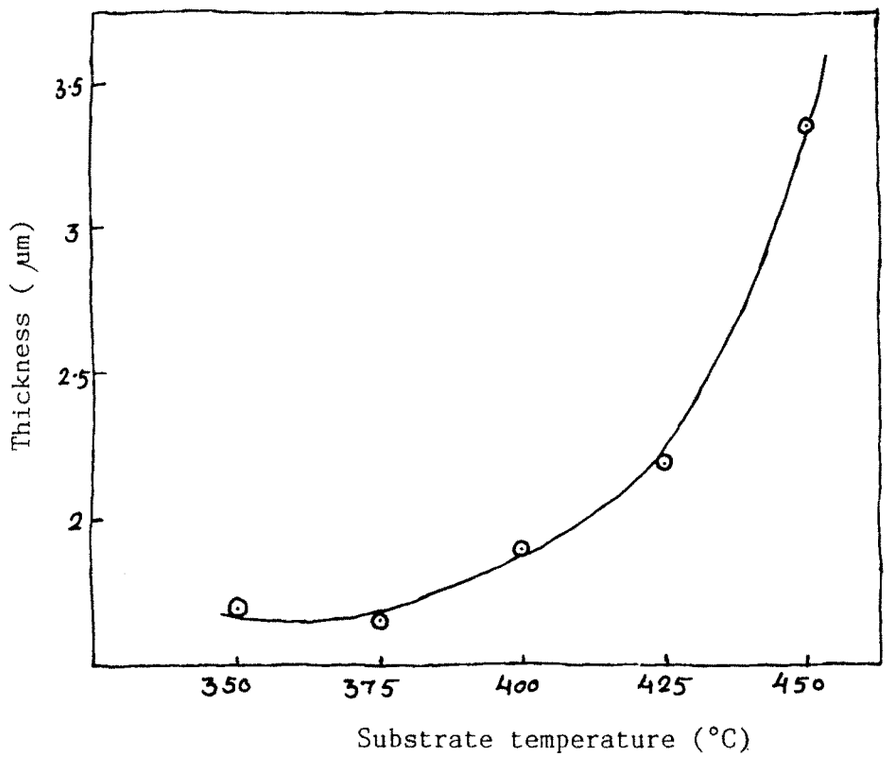

Fig. 5.12 Plot of film thickness versus substrate temperatures.

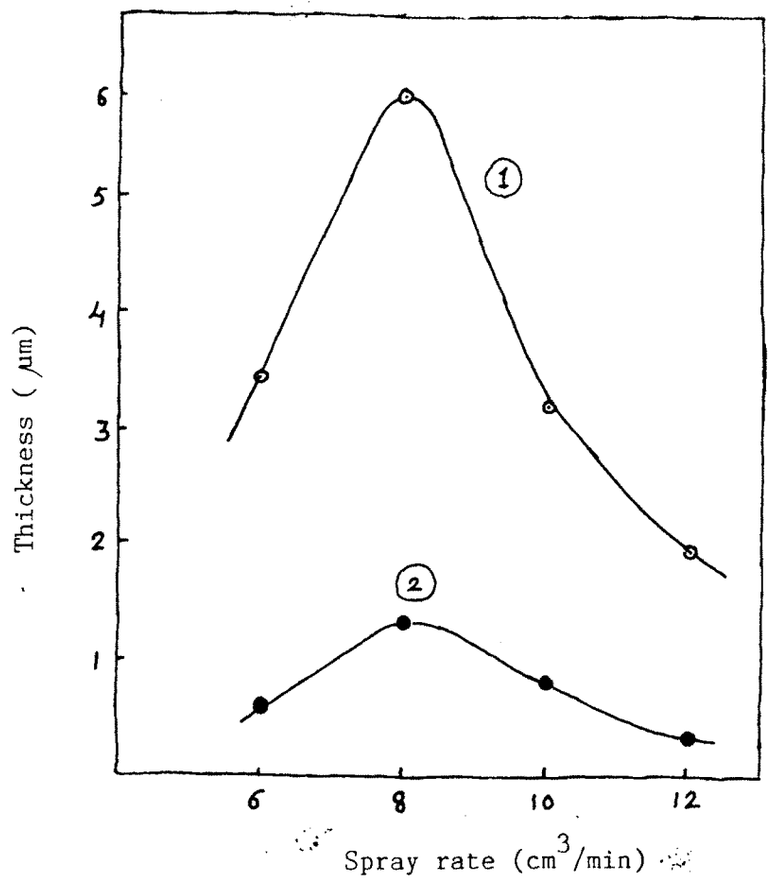

Fig. 5.13 Plot of film thickness versus spray rates for films prepared on (1) nonconducting (2) conducting glass substrates respectively.

film thickness with increase in spray rate beyond the particular spray rate may be attributed to increase in momentum and decrease in size of droplet. Due to large momentum the small droplet is sprayed out over a large area. The temperature is sufficient to evaporate the maximum part of the droplet. At the particular spray rate (8cc/min) the size and momentum are moderate so that the maximum portion of droplet remains on the glass substrate in the deposited condition.

It was found that the spray rate at which the thickness is maximum is not proper for deposition as the film deposited on conducting glass is not uniform. Though at 12 cc/min spray rate film thickness is less, the film is uniform on conducting as well as nonconducting glass substrate. For 0.25M concentration the film thickness is less than for higher concentration but conductivity is more as discussed before. Similarly for 400°c substrate temperature though the thickness is less crystallinity is better than higher substrate temperature films as discussed in chapter IV.

REFERENCES

1) M.D.Uplane, Ph.D. Thesis, Shivaji University, Kolhapur (1984).

2) C.D.Lokhande, Ph.D. Thesis, Shivaji University, Kolhapur(1983)

3) D.Adler and J.Feinleib, Phys. Rev.,B_2, 3112(1970).

4) R.Bharati, R.A.Singh and Y.P.Yadava, J.Mat.Sci.Let., 2, 623-24(1983).

5) A.L.Dawar, V.P.Taneja, Pratap Kumar and P.C. Mathur, Thin Solid Films, 79, 185-191(1981)

6) S.K.Sarkar, M.L.Sharma and S.K.Lahiri, J.Mat.Sci.Let., 6, 958-60(1987).

7) G.V.Subba Rao, B.M.Wanklyn and CNR Rao, J.Phys. Chem. Solids, 32, 345-58(1971)

8) Iginio Barbariol and Sergio Roitti, J.Mat.Sci.Let.,3, 181-83(1984).

9) Jaroslav Jerhot and Jaroslav Vicek, Thin Solid Films, 92, 259-271(1982).

10) E.J.W. Verwxy and J.H.Boer, Rec. Trav.Chim, 55, 531(1936).

11) F..Morin, Phys. Rev., 93, 6, 1199(1954).

12) G.P.Sykora and T.O.Mason,Mater Res.Soc.,243-9(1986).

13) M.D.Uplane and S.H.Pawar, Solar cells, 10, 177(1983).

14) Bodh Raj., D.K.Pandya and K.L.Chopra, Proceedings of National Solar Energy Convention, Allied Publishers, 7.001(1981).

15) M.D.Uplane and S.H.Pawar, Mat. Res. Bull., 5, 433-40 (1983).